Construction of targeting vectors and generation of mouse mutants

MT2-MMP (Genbank accession # NC_000074) specific sequences were cloned from a Lamda Fix 129 mouse genomic library (Stratagene, La Jolla, CA). For targeted deletion of MT2-MMP, a targeting vector containing a 4.7kb PstI/BamHI long homology comprising intron 1 sequences and part of exon 2 was cloned into NotI/BamHI restricted pKO924 using the phage polylinker NotI site next to the PstI site of the inserted fragment (Stratagene, La Jolla, CA). A 0.78 kb BglII/KpnI short homology fragment comprising part of intron 5, exon 6 and most of intron 7 was inserted into BglII/HpaI restricted vector following blunt ending of the KpnI overhang. The intervening sequence containing part of exon 2 through exon 5 was replaced with an AscI pgk-Neo cassette and the vector was finalized by inserting an HSV-tk cassette into the unique RsrII site of pKO924.

10^8 W4129S6 cells (Taconic, Germantown, NY) were electroporated with 50nM of NotI linearized targeting vector @ 800V/cm, 200µF and selected in DMEM, 15% FBS supplemented with 350µg/ml G418 (Invitrogen, Grand Island, NY) and 1000 U/ml Recombinant LIF (ESGRO) (Millipore, Billerica, MA). Resistant clones were picked, expanded and screened for homologous recombination into the MT2-MMP locus by digestion of DNA with SacI, fractionation on agarose gels, transfer to nylon membranes and hybridization to a PCR generated probe spanning intron 8 and exon 9 (oligos: fw: 5'-AACTGTATCCCTGTCCATCTTCTG-3′ rev: 5'-AAACCGCTCACCTGTCTGCTTG-3'). For routine screening of genotypes by PCR, the endogenous wildtype allele was amplified with the primers A: MT2ex4–1: 5′-CCTATGATGACATTCGGCTACG 3′ and B: MT2ex5 5′-GTTGTCGGTATCCATCCACTGGTAGAAGGGTGC 3′ and the targeted allele was detected using the primers D: MT2-Neo1 5′- TGAGCCCAGAAAGCGAAGGAGC 3′ AND C: MT2 Int1-2A 5′- TACCAGTCGGCAGGATGGAAGC 3′. Mice were generated as described [15] and bred to homozygosity. Ablation of functional messenger RNA from the gene was ascertained by RT-PCR using primers spanning exons 2–6, 2–7, and 2–8: (exon2: 5′-ATGCGCTCCTGGCTGCGGCTCTATGGCTACCTACCCC-3; Exon6: 5′-ATGTTGGGGCCATACTGGT-3′; Exon7: 5′-AATGTCCATCCTGGCGCTCGTAGGC-3′; Exon8; 5′-GTGTCAATGCGGTCATAGGG-3′). No product could be amplified from 2(−/−) mice as demonstrated in Fig. S1C.

For generation of the conditional MT1-MMP (Genbank Accession# NC_000080) allele, an 11.6 kb targeting vector was constructed by placing a reverse orientation PGK-Neo cassette flanked by Flippase Recombination Targets (FRT) and one locus of X over-P1 (LoxP) site 855 base pairs 5′- of exon 2. A second LoxP site was inserted 510 base pairs 5′- of exon 6 enabling excision of exon 2 through 5 following Cre-mediated recombination (Fig. S2). Mouse ES cells were targeted as described for generation of the MT2-MMP allele above and Bgl II/SstI restricted DNA was tested for legitimate recombination by Southern blot using a radiolabeled cDNA probe spanning the last 25 bp of exon 9 and all of exon 10. For routine genotyping of mice, the targeted allele including FRT sites and the upstream LoxP site was detected by PCR using primers A' (3′Neo341): 5′-CAGAAAGCGAAGGAGCCAAAGC-3′ and B:(3′13345) 5′-CACTGAGCTAAATTCCCAACCC-3′ generating a 500 bp product. The endogenous allele was detected using primers A:(5′-13109) 5′-TTCGCTACCACCCTAAAGAGCACAGC-3′ and B:(3′13345) 5′-CACTGAGCTAAATTCCCAACCC-3′ which generate a 236 bp product. The presence of a downstream LoxP site was ascertained using primers C (5′-16046): 5′-

CCATCCCCATTCCTGCTCCTCCA-3′ and D:(3′16518) 5′-AAGTTTGGTCCCCAGCACTCACA-3′ which generate a 510 bp product in the presence of the LoxP site and a 472 bp product from the endogenous allele. To excise the PGK-Neo cassette from the targeted gene heterozygous mice were bred to the Flipper mouse, 129S4/SvJaeSor-Gt(ROSA)26Sortm1(FLP1)Dym/J (Jackson Laboratories, Bar Harbor, ME) Stock # 003946 as outlined in Fig. S2A. The flipped allele (1^{LoxP}) and the recombination was verified by PCR using primers A and B. Presence of the FRT/LoxP array in the template yielded a 350 bp product whereas the equivalent wildtype allele produced a 236 bp product. Mice with this 1^{LoxP} allele were subsequently crossed to MT2-MMP deficient mice ($2^{-/-}$) or mated to the mice carrying a null allele for MT1-MMP ($1^{-/-}$) [16] or any relevant allelic combination thereof. To excise the intervening sequences between LoxP sites and render the 1^{LoxP} allele non-functional, mice were crossed to Tg(cre/Esr1)5Amc/J mice (Jackson Laboratories, Bar Harbor, ME) Stock# 004453 and administered Tamoxifen as outlined later in the materials section. Recombination of the floxed locus was confirmed by PCR using primers A:(5′-13109) 5′-TTCGCTACCACCCTAAAGAGCACAGC-3′ and E:(3′16675) 5′-GGTTCCCAGAGCCGACAA-3′ which generate a 590 bp product. The MT1-MMP mRNA level following recombination was established by real time PCR on tissue as outlined later in this section. Cre-transgenic mice were identified by PCR using the primers: Cre Up: 5′-GGACATGTTCAGGGATCGCCAGGCG-3′ and Cre Down: 5′-GCATAACCAGTGAAACAGCATTGCTG-3′

Expression RNA microarray analysis

Fetal portions of the placentas were dissected and DNase-free RNA was prepared using an RNAqueous-4PCR kit (Ambion, Inc., TX) according to the manufacturer's protocol.

Complementary fluorescent RNA for use with Agilent's oligonucleotide microarrays was generated from 1µg of total RNA using Agilent Low RNA Input Amplification Kit (Agilent Technologies, Santa Clara, CA). To provide a positive control for monitoring the microarray workflow, RNA samples were spiked with control RNA from Agilent One Color RNA Spike-In Kit (Agilent Technologies, Santa Clara, CA) according to the manufacturer's protocol. Labeled and amplified RNA was purified using Qiagen RNeasy mini spin columns (Qiagen, Valencia, CA) and hybridized to 1 × 44K Whole Mouse Genome Microarrays (Cat. # G4122F Agilent Technologies, Santa Clara, CA) for 17 hours at 65°C using a Gene Expression Hybridization Kit (Agilent Technologies, Santa Clara, CA). Microarray slides were scanned on an Agilent Microarray Scanner and the data were extracted using Agilent Feature Extraction Software. Analysis of the data was performed using GeneSpring GX 9 software. Array data can be retrieved using GEO accession # GSE18604.

Confocal Microscopy

Acquired Z-stacks were reconstructed into 3D volumes and analyzed using Volocity software (Perkin Elmer, Coventry, UK). Briefly, intensity thresholds were set between 10 and 255. For areas and sum fluorescence in the allantoic mesenchyme, the software was set for selection of contiguous signals greater than 4×10^5 voxels. For peri-vascular mean fluorescence intensity measurements, 42 sample points were identified in the vascular periphery and fluorescence values were acquired.

Mass spectrometry analysis
The fetal portions of the placentas from E10.5 embryos were dissected and processed for mass spectrometry analysis as described [33].

Whole mount preparation of mammary glands
Age matched ($1^{loxP}/-$; $2-/-$); Cre+ and ($1^{loxP}/-$; $2-/-$); Cre-lactating females were dosed with tamoxifen 5 times as described previously and the pups were weaned following treatment. Seven days after weaning, mammary glands were collected and stained with carmine red as described.[24] MT1-MMP expression was analyzed as described previously in the materials section and contra lateral glands were processed, sectioned and stained with H&E.

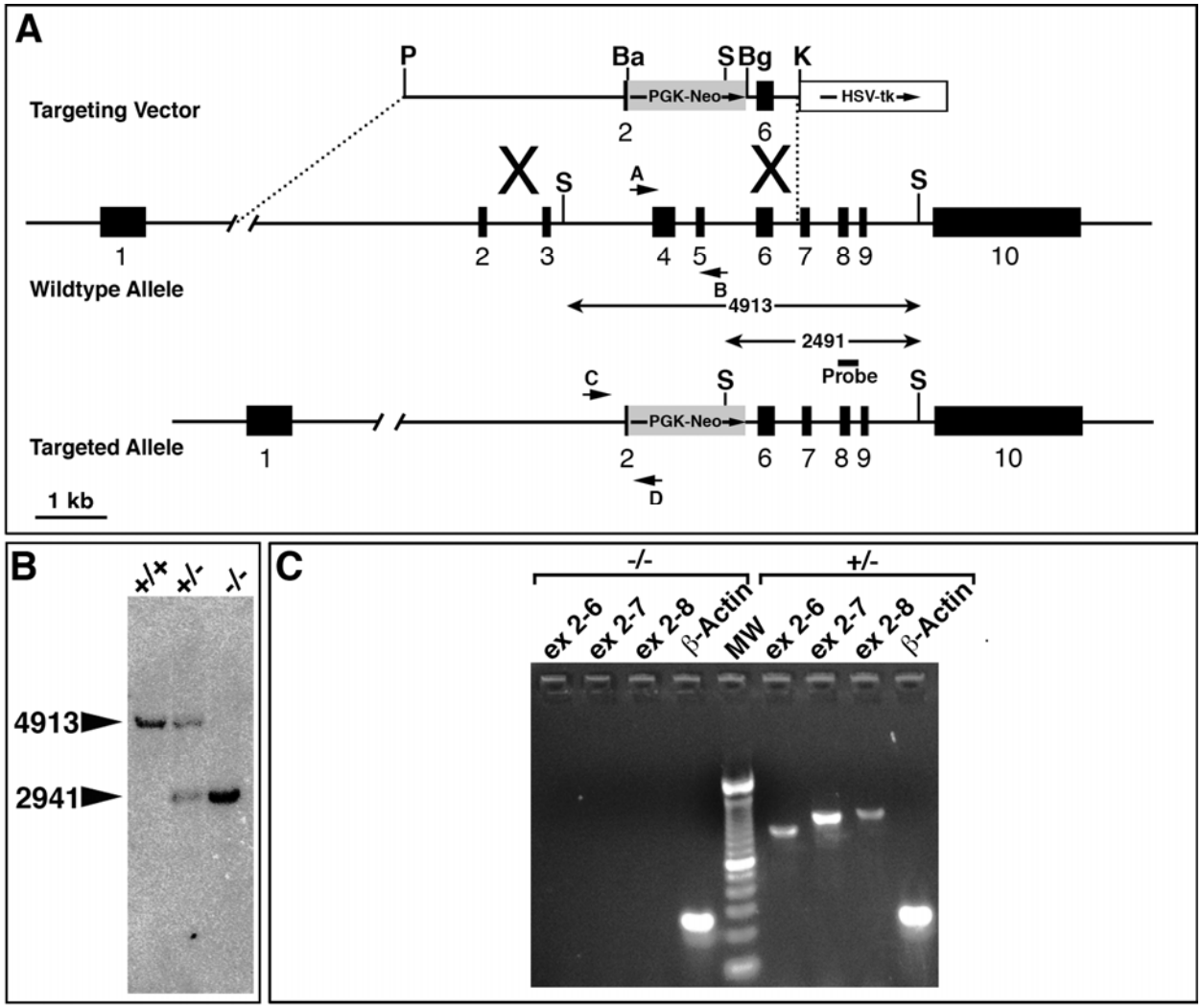

Figure S1. Strategy for MT2-MMP targeting and loss of MT2-MMP mRNA
(A) Targeting strategy for the mouse MT2-MMP allele. Non-coding sequence is depicted as solid black lines, exons as solid black boxes. The PGK-Neo cassette is shown in grey and the HSV-tk cassette as a white box. “A” and “B” indicate location of primers used for detection of the wildtype MT2-MMP allele. “C” and “D” indicate the location of primers used for detection of the targeted allele. Targeting removes sequences from the 3′ end of exon 2 through exon 5 and eliminates the catalytic site of MT2-MMP. Ba, BamHI; Bg, BglII; K, KpnI; P, PstI; S, SstI. (B) Southern blot with the probe delineated in (A) verifying disruption of the MT2-MMP gene. Wildtype allele (4913 bp band) and targeted allele (2941 bp band). (C) RT-PCR for MT2-MMP confirming the ablation of messengerRNA in MT2-MMP knockout embryo compared to the control littermate.

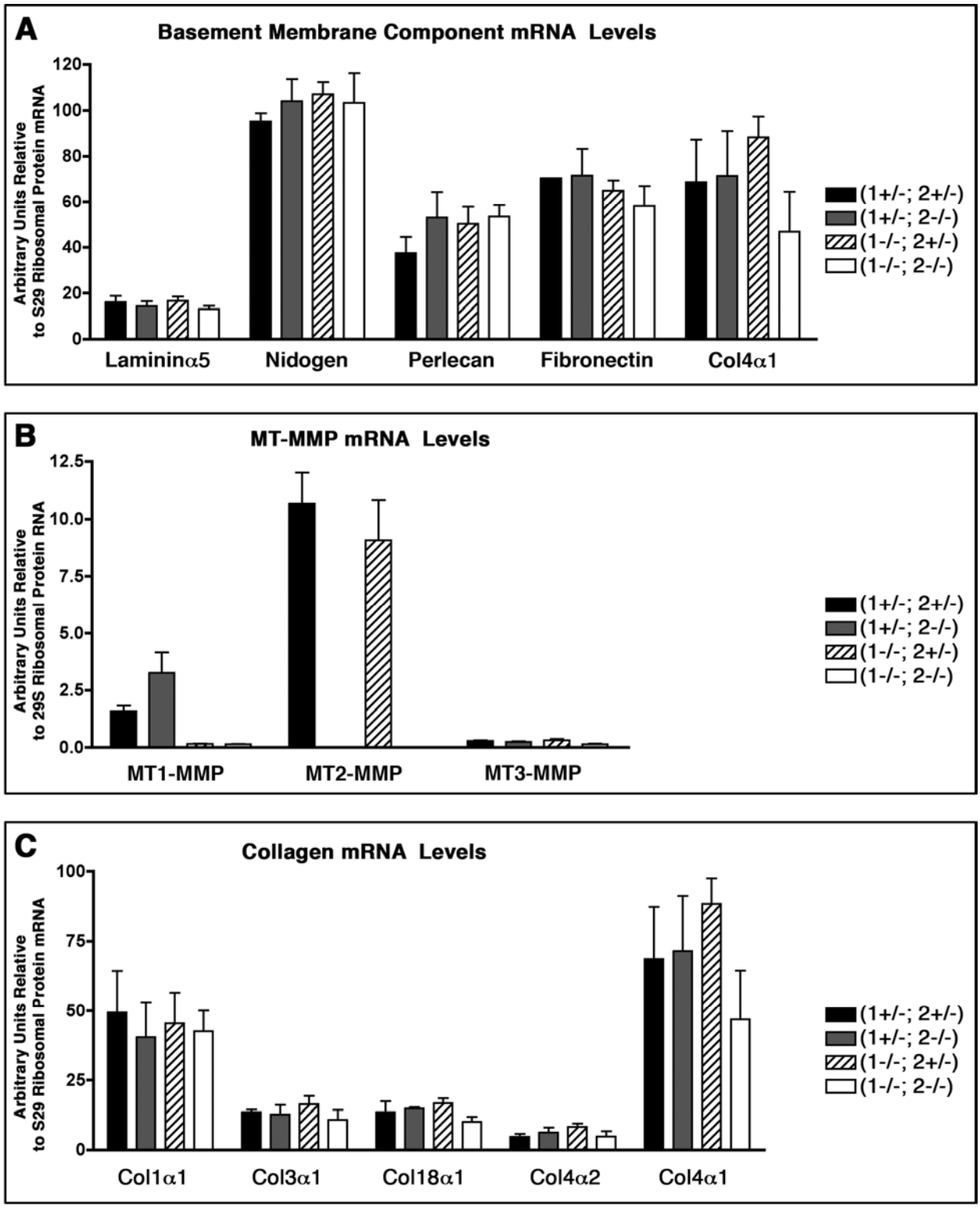

Figure S2. mRNA levels of extracellular matrix molecules and MT-MMPs in fetal placental tissue

(A) mRNA levels of basement membrane components determined by real time PCR as a function of placenta genotype at E10.5. (B) MT-MMP mRNA levels for MT1-, MT2-, and MT3-

MMP as a function of placental genotype (C) mRNA levels of various collagen chains as a function of genotype. Gene expression for the various molecules analyzed did not differ in response to loss of MT1-MMP and MT2-MMP. No compensatory expression of MT3-MMP was detected.

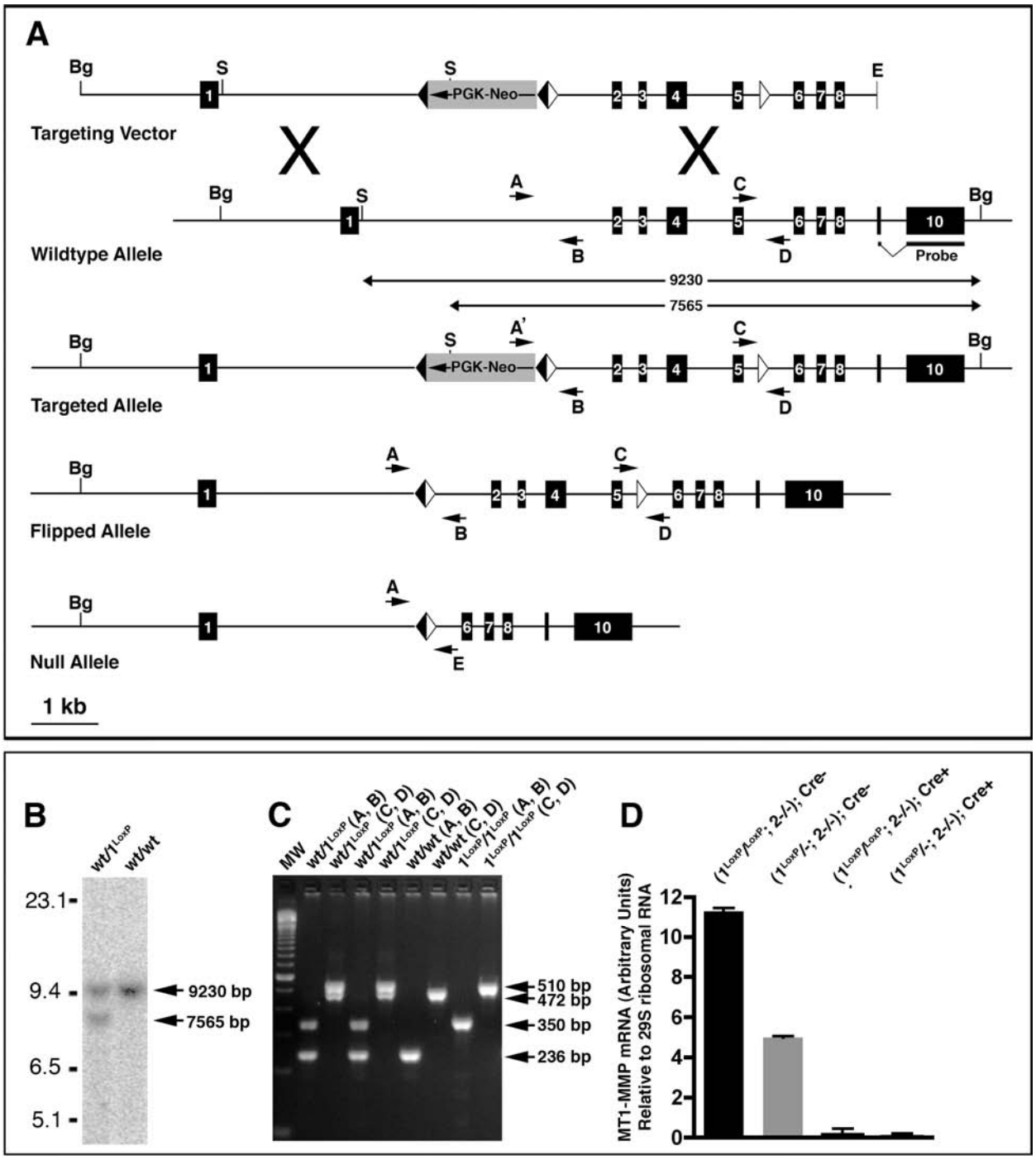

Figure S3. Strategy for conditional deletion of MT1-MMP

(A) Schematic representation of the strategy for conditional deletion of the MT1-MMP allele. Non-coding sequence is depicted as solid black lines and exons as solid black boxes. The PGK-Neo cassette is shown in grey. Flippase Recombination Target (FRT) sites are depicted as solid black triangles and locus of X over-P1 (LoxP) sites are depicted as open white triangles. “A”, “A’”, “B”, “C”, “D” and “E” indicate the location of primers used for genotyping as shown in (C). Bg, BglII; E, EcoRI; S, SstI. (B) Southern blot detection of the endogenous (9230bp band) and targeted floxed (7565bp band) of the MT1-MMP allele. (C) Agarose gel electrophoresis of

PCR product for detection of alleles outlined in (A). (D) Relative levels of MT1-MMP mRNA measured by real-time PCR in mouse tissue following tamoxifen induced ablation of the (flipped) floxed MT1-MMP allele with tamoxifen inducible Cre-recombinase.

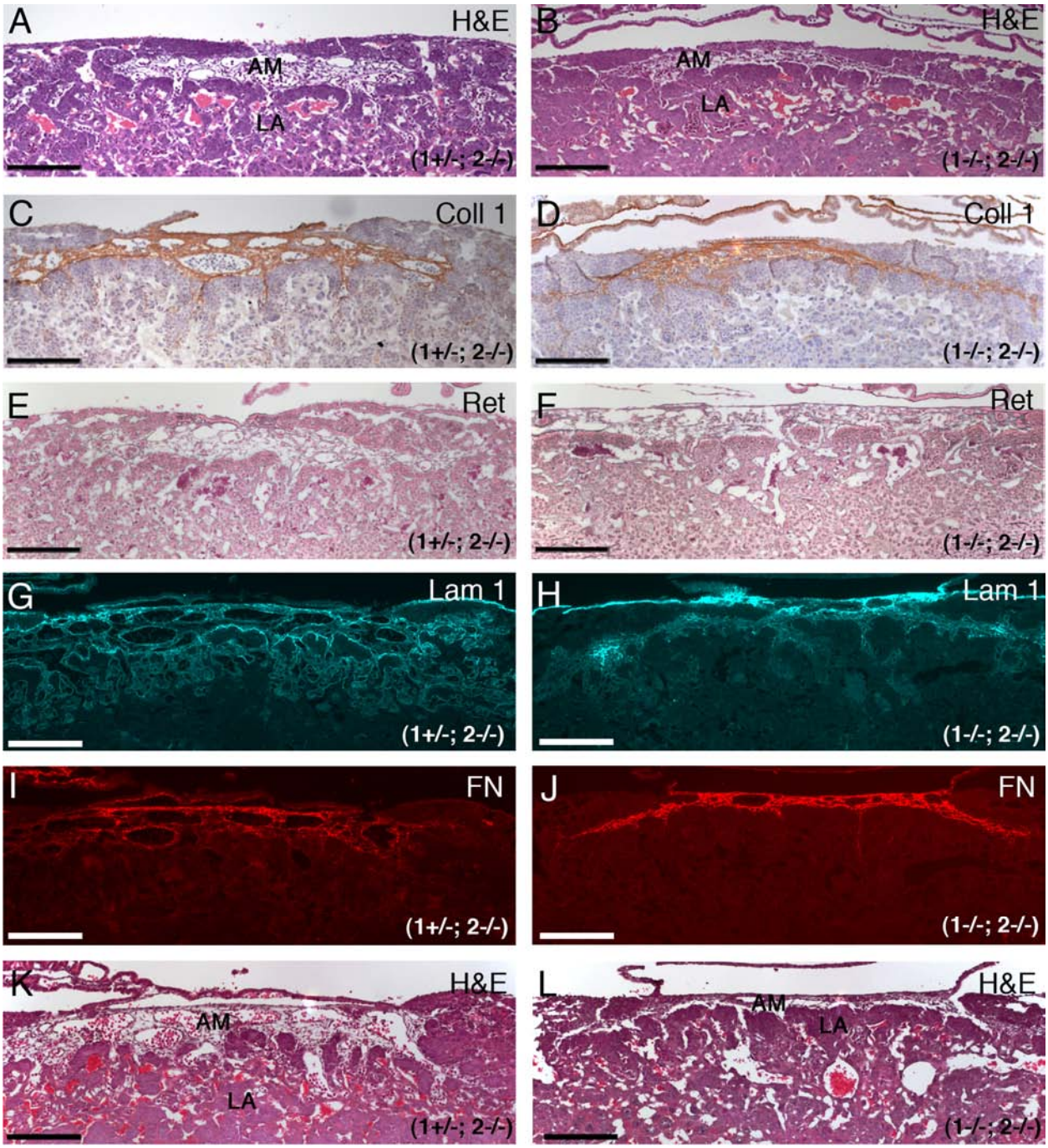

Figure S4. Extracellular matrix distribution in MT1-MMP/MT2-MMP-deficient placentas
(A) H&E stained cross section of E10.5 day control placenta and (1−/−; 2−/−) double-deficient placenta (B) showing allantoic mesenchyme (AM) and labyrinth (LA). (C) and (D), sections serial with those in a (A) and (B) reacted with antibody specific for collagen type I (brown stain). (E and F), other sections demonstrating reticulin fiber stain (black). This type III collagen-rich matrix is restricted mostly to the allantoic mesenchyme. (G and H), Immunofluorescent sections reacted with laminin-1 specific antibody (cyan). (I and J), serial sections reacted with antibody specific for fibronectin (red). (K and L) serial sections to G, I and H, J stained with H&E. The

staining patterns demonstrate that extracellular matrix components are predominantly located in the allantoic mesenchyme and to a lesser extent associated with fetal vessels in the labyrinth. Because of this peri-vasculature distribution, there is a distinct reduction in staining of the prospective labyrinth following loss of MT1-MMP and MT2-MMP, compare (D, H and J) to (C, G, and I). Scale bar A-I: 200μm.

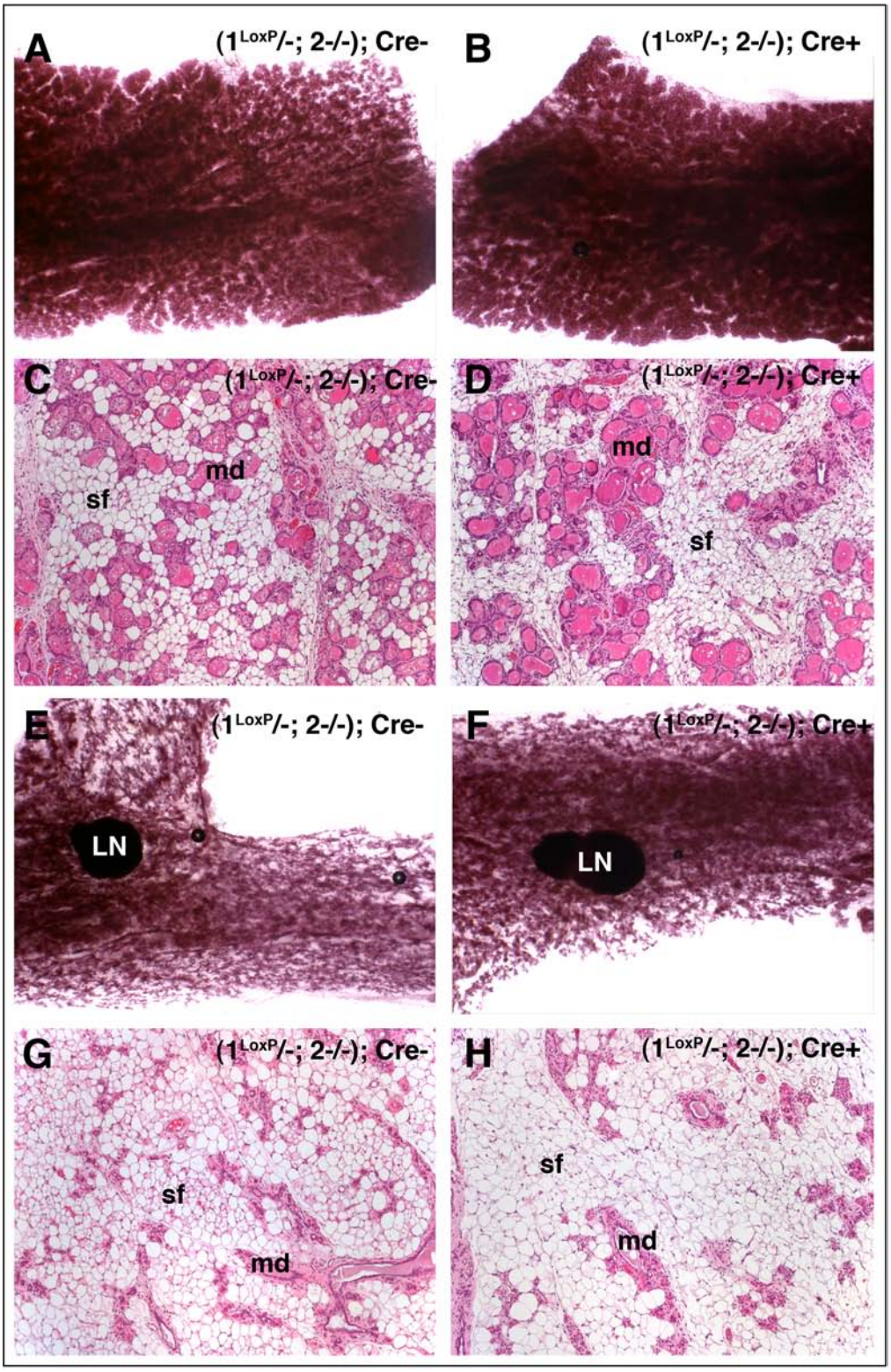

Figure S5. Loss of MT1-MMP and MT2-MMP does not affect mammary gland involution
(A) Carmine red stained whole-mount preparation of early involuting mammary gland from (1^{Loxp}/-; 2–⁄–); Cre- mouse treated with tamoxifen prior to weaning of pups. The gland still

retains gross alveolar appearance. (B) Carmine red whole mount stain of involuting mammary gland from (1^{Loxp}/-; 2−/−); Cre+ mouse treated as in (A) displaying the same morphology as shown in (A). (C) H&E section of the contra-lateral gland from the animal shown in (A) note the abundance of mammary ducts (md) dispersed in the stromal fat pad (sf). The gland still retains the alveolar structure characteristic of a lactating or post-lactating gland. (D) H&E section of the contra-lateral gland from animal shown in (B). Note the gland displays the same morphology as seen in (C). (E) Carmine red stained whole-mount preparation of later stage involuting mammary gland from (1^{Loxp}/-; 2−/−); Cre- mouse treated with tamoxifen prior to weaning of pups. Note the alveolar architecture is gone indicating an advanced stage of the involution process. (F) Carmine red whole-mount stain of later stage involuting mammary gland from (1^{Loxp}/-; 2−/−); Cre+ mouse treated with tamoxifen prior to weaning of pups. Note the gland displays similar morphology as seen in (E) suggesting that involution proceeds unimpeded in the absence of MT1-MMP and MT2-MMP. (G) H&E section of the contra-lateral gland from the animal shown in (E). Note the rare ducts (md) dispersed in the stromal fat pad (sf) with no evidence of the prior alveolar duct structure. (H) H&E section of the contra-lateral gland from the animal shown in (F). The gland displays the same structure as that seen in (G) indicating that the loss of MT1-MMP and MT2-MMP is compatible with mammary gland involution.

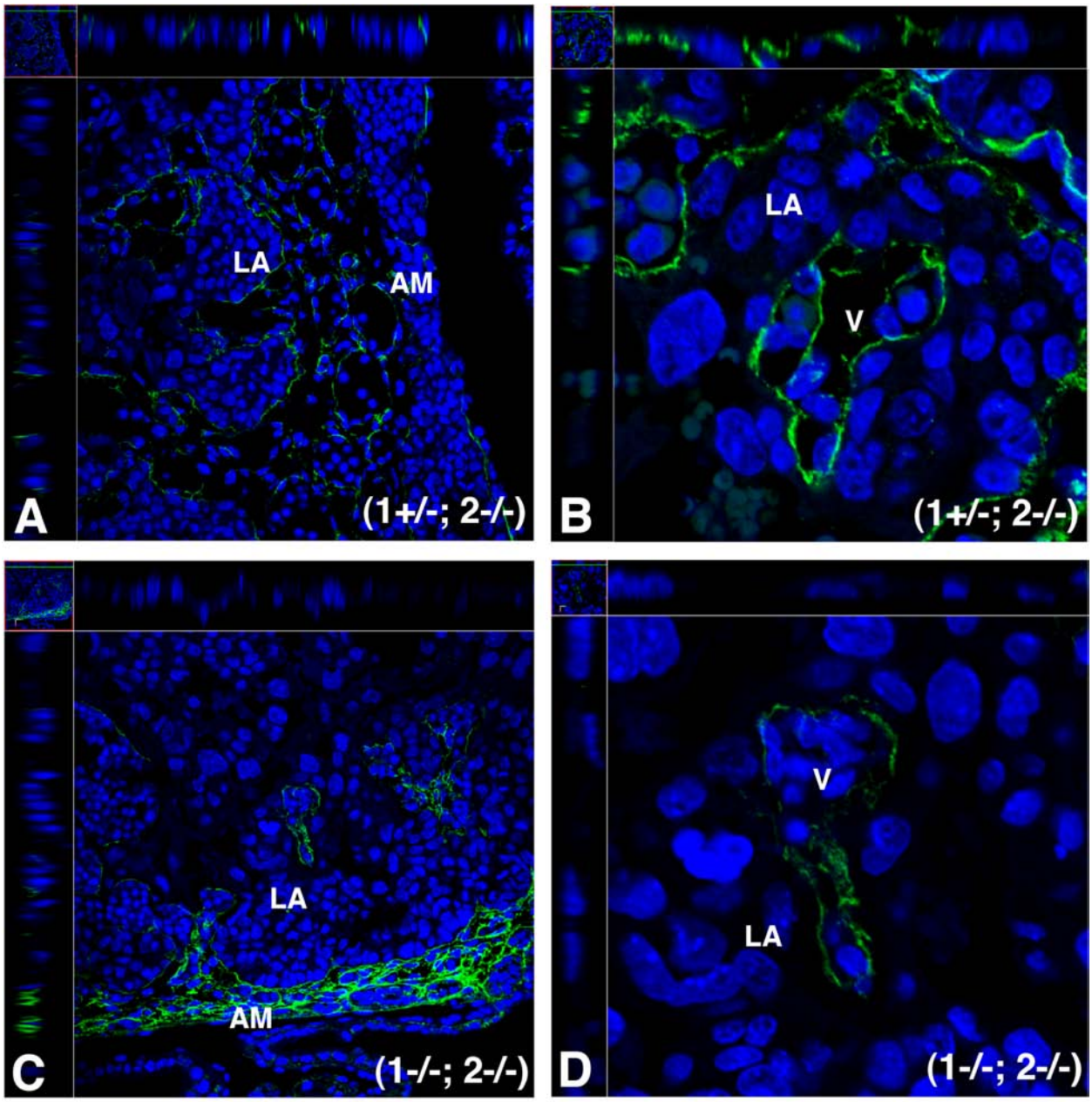
A
LA
AM
(1+/-; 2-/-)
B
LA
V
(1+/-; 2-/-)
C
LA
AM
(1-/-; 2-/-)
D
V
LA
(1-/-; 2-/-)

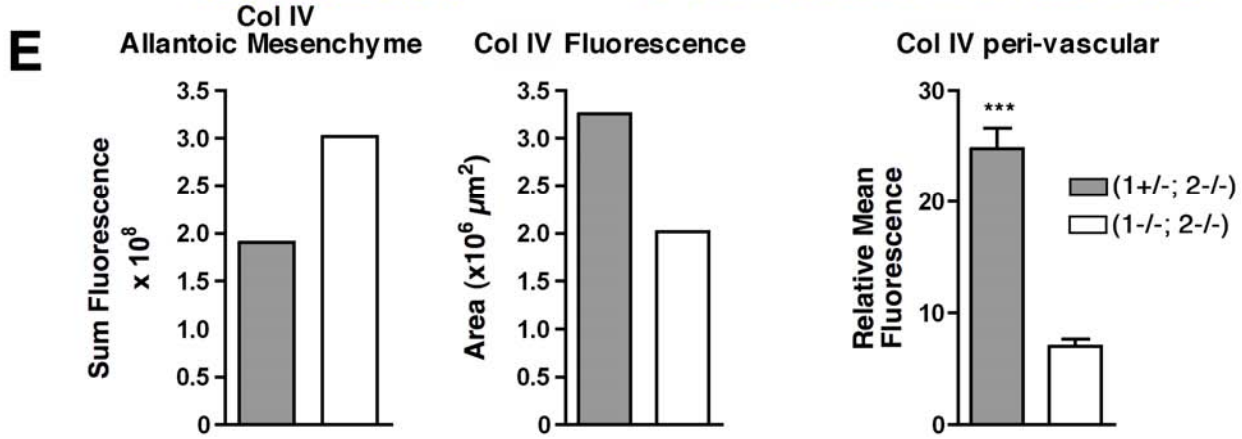
E
Col IV
Allantoic Mesenchyme
Sum Fluorescence
x 10^8
3.5
3.0
2.5
2.0
1.5
1.0
0.5
0
Col IV Fluorescence
Area (x10^6 μm^2)
3.5
3.0
2.5
2.0
1.5
1.0
0.5
0
Col IV peri-vascular
Relative Mean
Fluorescence
30
20
10
0
***
(1+/-; 2-/-)
(1-/-; 2-/-)

Figure S6. Immunolocalization of type IV collagen
(A) Confocal micrograph of placenta from (1+/−; 2−/−) mouse demonstrating type IV collagen in the allantoic mesenchyme (AM). Note that most staining is restricted to the labyrinth (LA). (B) High power image of a single vessel (V) in the labyrinth from (1+/−; 2−/−) mouse demonstrating perivascular localization of type 4 collagen. (C) Confocal micrograph of placenta from (1−/−; 2−/−) mouse demonstrating type 4 collagen in the allantoic mesenchyme (AM). Note that most staining is restricted to the allantoic mesenchyme (AM) as opposed to the control (A) where staining is predominant in the labyrinth (LA). (D) High power image of a single vessel from the prospective labyrinth of a (1−/−; 2−/−) placenta. Note the comparative reduction of staining relative to (B) suggesting that matrix accumulation around the vessels is not taking place at the same rate as in the control tissue. (E) quantification of the type IV collagen in the allantoic mesenchyme and in labyrinth vessels.

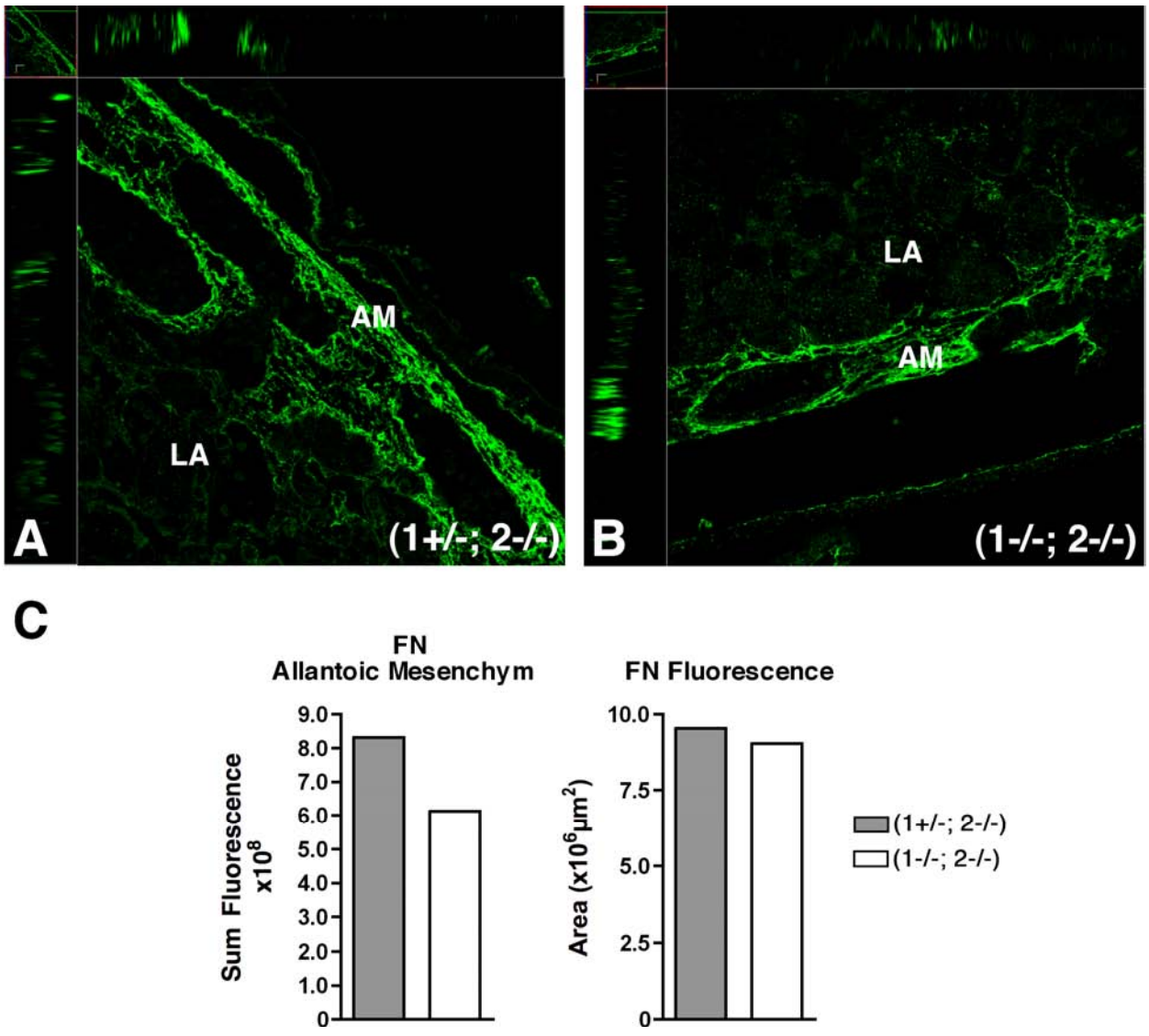

Figure S7. Immunolocalization of fibronectin

(A) Confocal micrograph of placenta from (1+/–; 2–/–) mouse demonstrating fibronectin in the allantoic mesenchyme (AM). Note that most staining is restricted to the allantoic mesenchyme at this stage (AM). (B) Confocal micrograph of placenta from (1–/–; 2–/–) mouse demonstrating fibronectin in the allantoic mesenchyme (AM). As seen in (A) most staining is restricted to the allantoic mesenchyme (AM). Note the comparative levels of staining in both panels. (C) quantification of the fibronectin in the allantoic mesenchyme. The level of staining around vessels in the labyrinth does not allow for quantification at this stage as seen for type IV collagen and laminin.

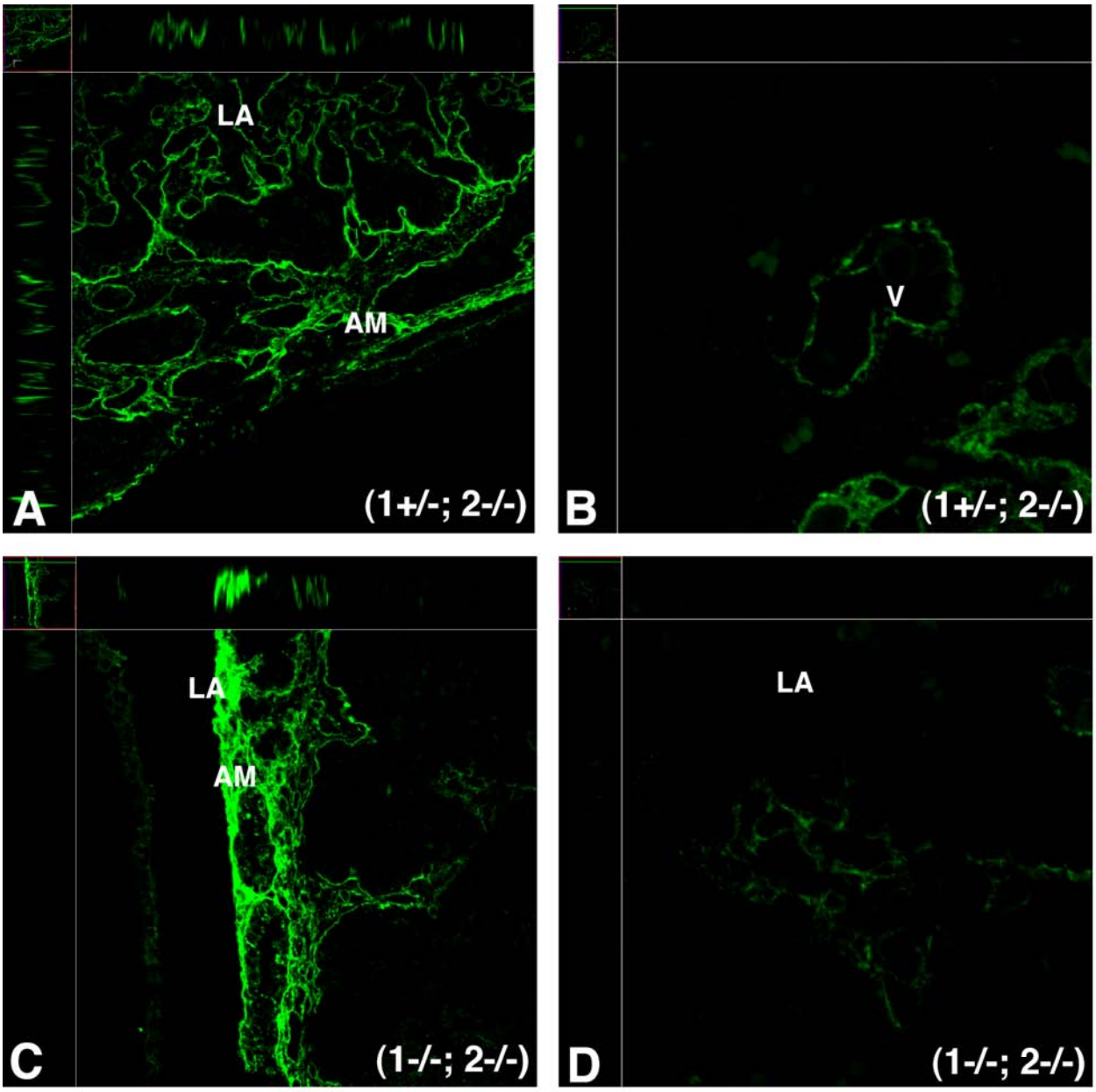
LA
AM
A
(1+/-; 2-/-)
V
B
(1+/-; 2-/-)
LA
AM
C
(1-/-; 2-/-)
LA
D
(1-/-; 2-/-)

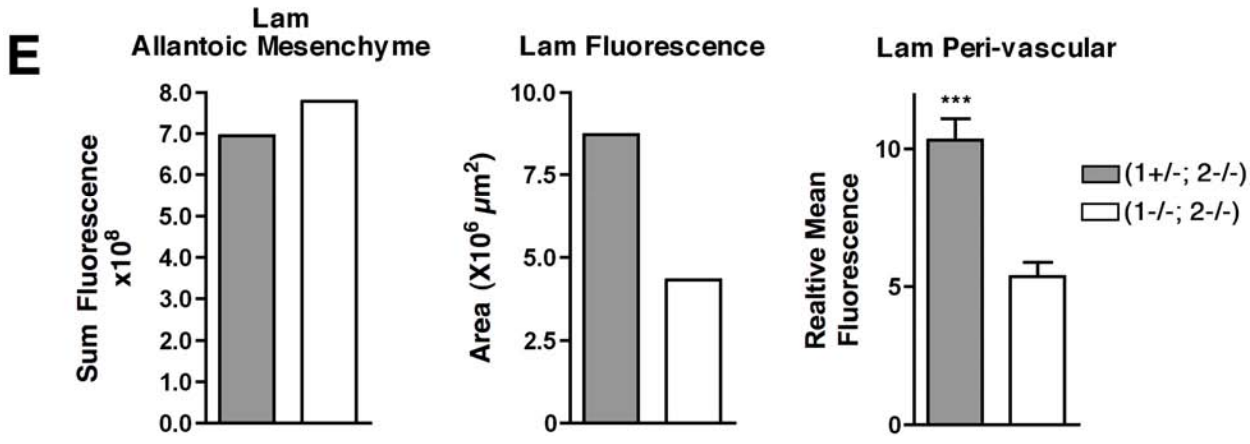
E
Lam
Allantoic Mesenchyme
Sum Fluorescence
x10^8
8.0
7.0
6.0
5.0
4.0
3.0
2.0
1.0
0.0
Lam Fluorescence
Area (X10^6 μm^2)
10.0
7.5
5.0
2.5
0
Lam Peri-vascular
Realtive Mean
Fluorescence
***
10
5
0
(1+/-; 2-/-)
(1-/-; 2-/-)

Figure S8. Immunolocalization of laminin

(A) Confocal micrograph of placenta from (1+/−; 2−/−) mouse demonstrating laminin in the allantoic mesenchyme (AM). Note that most staining is restricted to the labyrinth (LA). (B) High power image of a single vessel (V) in the labyrinth from (1+/−; 2−/−) mouse demonstrating perivascular localization of laminin. (C) Confocal micrograph of placenta from (1−/−; 2−/−) mouse demonstrating laminin in the allantoic mesenchyme (AM). Note that most staining is restricted to the allantoic mesenchyme (AM) as opposed to the control (A) where staining is predominant in the labyrinth (LA). (D) High power image of a single vessel from the prospective labyrinth of a (1−/−; 2−/−) placenta. Note the comparative reduction of staining relative to (B) suggesting that matrix accumulation around the vessels is not taking place at the same rate as in the control tissue. (E) quantification of the laminin in the allantoic mesenchyme and in labyrinth vessels.